Earth Planets Space, **64**, 1259–1266, 2012

Long-term change of site response after the M_w 9.0 Tohoku earthquake in Japan

Chunquan Wu[1] and Zhigang Peng[2]

[1]*Geophysics Group (EES-17), Los Alamos National Laboratory, Los Alamos, NM 87545, U.S.A.*
[2]*School of Earth and Atmospheric Sciences, Georgia Institute of Technology, Atlanta, GA 30332, U.S.A.*

(Received December 27, 2011; Revised May 6, 2012; Accepted May 17, 2012; Online published January 28, 2013)

The recent M_w 9.0 off the Pacific coast of Tohoku earthquake is the largest recorded earthquake in Japan's history. The Tohoku main shock and its aftershocks generated widespread strong shakings as large as ∼3000 Gal along the east coast of Japan. Wu and Peng (2011) found clear drop of resonant frequency of up to 70% during the Tohoku main shock at 6 sites and correlation of resonance (peak) frequency and peak ground acceleration (PGA) during the main shock. Here we follow that study and systematically analyze long-term changes of material properties in the shallow crust from one year before to 5 months after the Tohoku main shock, using seismic data recorded by the Japanese Strong Motion Network KiK-Net. We use sliding window spectral ratios computed from a pair of surface and borehole stations to track the temporal changes in the site response of 6 sites. Our results show two stages of logarithmic recovery after a sharp drop of resonance frequency during the Tohoku main shock. The first stage is a rapid recovery within several hundred seconds to several hours, and the second stage is a slow recovery of more than five months. We also investigate whether the damage caused by the Tohoku main shock could make the near surface layers more susceptible to further damages, but we do not observe clear changes in susceptibility to further damage before and after the Tohoku main shock.
Key words: Tohoku earthquake, earthquake ground motion, site effects, wave propagation, soil nonlinearity, KiK-Net.

1. Introduction

It has long been recognized that the amplitude of seismic waves approaching the Earth's surface is amplified by passing through soil layers with low impedance (e.g., Joyner *et al*., 1976; Chin and Aki, 1991; Yu *et al*., 1992). When the strong ground shaking exceeds a certain threshold, the soil response deviates from the linear Hooke's law, resulting in nonlinear site effects (e.g., Wen, 1994; Beresnev and Wen, 1996). The typical manifestation of nonlinear site response is a sharp reduction of the shear modulus (G) and quality factor (Q) of the sedimentary layers during strong shaking. Recent studies also found logarithmic recovery of the material properties with a wide range of time scale (seconds to years) after large earthquakes (Sawazaki *et al*., 2006, 2009; Wu *et al*., 2009a, b, 2010; Rubinstein, 2011). Improved understanding of nonlinear site response during strong shaking and the subsequent recovery process is critical for estimating seismic hazard and predicting strong ground shakings caused by future large earthquakes (Frankel *et al*., 2002).

The 03/11/2011 M_w 9.0 off the Pacific coast of Tohoku earthquake is the largest earthquake in Japan over the past hundred years. This great earthquake is recorded by ∼1200 K-Net/KiK-Net strong motion seismic stations with peak ground acceleration (PGA) as high as ∼3000 Gal (Hirose *et al*., 2011). Several recent studies have shown evidence of soil nonlinearity at various sites in Japan during the Tohoku main shock (e.g., Bonilla *et al*., 2011; Nakata and Snieder, 2011; Wu and Peng, 2011). In particular, both Wu and Peng (2011) and Nakata and Snieder (2011) found apparent logarithmic recovery after the Tohoku main shock. However, the soil properties still did not recover to the level before Tohoku earthquake at the time when these studies were conducted. So it is not clear whether longer-term recovery exists, or some permanent change occurs and the soil properties never return to the pre-main shock level. In addition, previous studies have suggested that pre-existing damage caused by large earthquakes could increase susceptibility to further damage by moderate aftershocks (e.g., Rubinstein and Beroza, 2004b). Whether the Tohoku main shock makes the surface material more susceptible to damage remains to be investigated.

The Tohoku main shock occurred in a region with ample background seismicity. In particular, the main shock was preceded by an M_w 7.3 foreshock (and a few $M_w \geqq 6$ events) a few days before, and was followed by many $M_w \geqq 6$ aftershocks (Hirose *et al*., 2011). The rigorous foreshock/aftershock sequence was well-recorded by the nearby K-Net/KiK-Net stations. This provides an ideal dataset to quantify long-term temporal changes of the site response after the Tohoku main shock, and test the hypothesis of preexisting damage increasing susceptibility to further damage (Rubinstein and Beroza, 2004b).

doi:10.5047/eps.2012.05.012

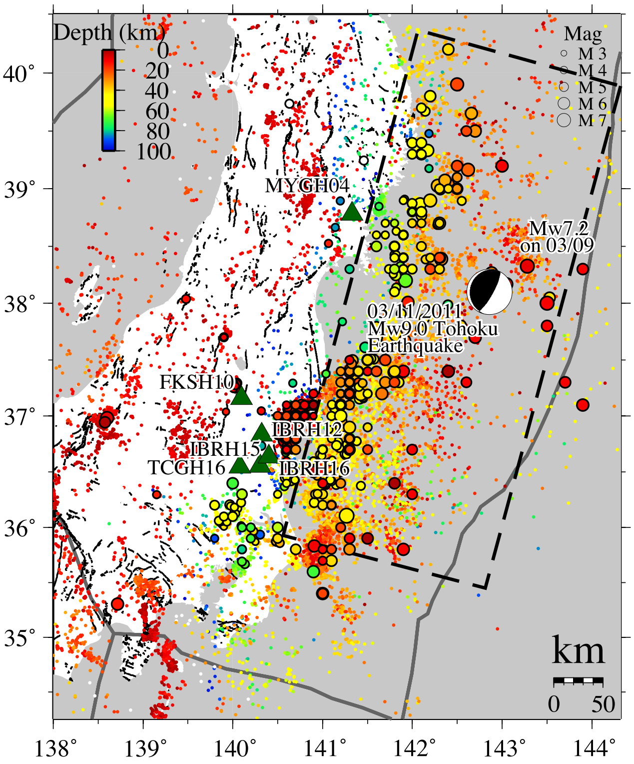

Fig. 1. Map of the study region in Japan. The epicenter of the 2011 M_w 9.0 Tohoku earthquake is indicated by the moment tensor solution (beach ball symbol). The large, black rectangle represents the fault area of the 2011 Tohoku earthquake, projected on the surface (Suzuki *et al.*, 2011). Epicenters of other events analyzed in this study are shown in large circles. The size of circle indicates the magnitude of each event and color shows the depth with red being shallow and blue being deep. The background events since 2011/01/01 from the Japan Meteorological Agency (JMA) catalog are shown as small dots. Locations of the 6 KiK-Net stations used in this study are shown in green triangles. The black lines show the active faults in this region and the grey lines denote the subduction plate boundaries.

2. Data and Analysis Procedure

2.1 Seismic data

Here we conduct a follow-up study of Wu and Peng (2011) utilizing the newly available strong motion data recorded by the Japanese Digital Strong-Motion Seismograph Network KiK-Net from 15 months before to 5 months after the Tohoku main shock. The KiK-Net is operated by National Research Institute for Earth Science and Disaster Prevention and consists of 659 pairs of surface/borehole strong-motion seismometers (Aoi *et al.*, 2000). Each KiK-Net unit is equipped with three-component accelerometers and a data logger having a 24 bit analog-to-digital converter with a sampling frequency of 100 Hz. Additional details on the network and site conditions can be found at the KiK-Net website (http://www.kik.bosai.go.jp).

Following Wu and Peng (2011), we analyze data recorded by six stations: FKSH10, IBRH12, IBRH15, IBRH16, MYGH04, and TCGH16 (Fig. 1). We focus on these six stations mainly because the observed temporal changes in resonance (peak) frequencies at these stations are much clearer than those at other stations (Wu and Peng, 2011), allowing us to better quantify long-term subtle temporal changes after the Tohoku main shock. In addition, the velocity contrasts between the surface soil layers and the underlying bedrocks are relatively stronger than those at other nearby KiK-Net stations (Fig. 2). Specifically, the alluvium and shallow sedimentary rocks in the top several tens of meters of these sites are generally clay, sandy clay, filling, and gravel with very low S-wave velocities of $\sim$100–200 m/s. The underlying bedrock types are typically conglomerate, argillite, and shale with S-wave velocities of $\sim$700–3000 m/s. The origin time of the rocks ranges from Jurassic to Palaeogene, Neogene, and Quaternary periods.

In the subsequent analysis we utilize a total of 457 events that occurred between 01/01/2010 and 08/31/2011 and recorded by the 6 surface/borehole strong motion sensors (Fig. 1). These include 103 events starting 15 months before, the Tohoku main shock, and 354 events within 5 months after the main shock. The magnitudes of the events range from 3 to 9, and the hypocentral depths range from 5 to 100 km. The maximum acceleration is 1220 Gal recorded at station FKSH10 during the Tohoku main shock.

2.2 Analysis procedure

The analysis procedure generally follows those of Wu and Peng (2011), and is briefly described here. We use 6-s sliding windows that are moved forward by 2 s at each step for all the waveforms recorded by the surface and borehole stations. The PGA value is then measured for each window. Note that here the term PGA refers to the maximum acceleration value in each window, rather than for the entire seismic records. We apply a sliding-window-based approach to the records of the Tohoku aftershock sequence to track the post-seismic changes of the resonance frequencies, and also to all the other events before the Tohoku main shock to measure the reference level (see the Results section). In our approach all possible seismic phases, including pre-event noise, P, S and coda waves are analyzed together. This is because previous studies based on the sliding window technique have found that the source and path effects are largely cancelled out by taking the spectral ratio (e.g., Sawazaki *et al.*, 2006; Wu *et al.*, 2009a).

Next, we remove the mean value of the traces and apply a 5 per cent Hanning taper to both ends. The power spectra of the two horizontal components are added up and then we take the square root of the sum to get the amplitude of the vector sum of the two horizontal spectra. The obtained spectra are then smoothed by computing the mean with half width of five points using the subroutine "smooth" in the Seismic Analysis Code (Goldstein *et al.*, 2003). The spectral ratio is obtained by taking the ratio of the horizontal spectra for the surface and borehole stations.

3. Results

3.1 General observations

Figure 3 shows an example of analysis procedure for the acceleration records at station IBRH15 generated by an M_w 7.0 aftershock of Tohoku earthquake occurred on 04/11/2011. The resonance frequency and the peak of the spectral ratio for the direct S wave clearly shift to lower values when comparing with those for the pre-event noise and coda-wave windows, suggesting the existence of nonlinear site response during this aftershock.

After processing all the data, we obtain $\sim 10^5$ spectral ra-

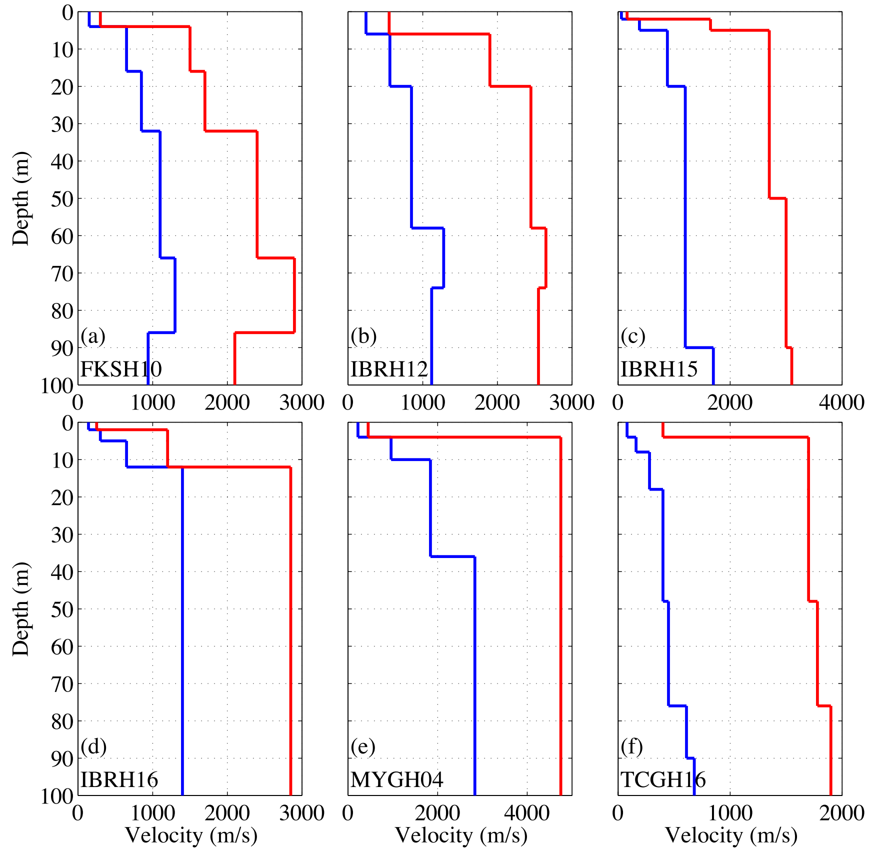

Fig. 2. Velocity profiles of the six sites analyzed in this study. The red and blue lines show the P- and S-wave velocities, respectively.

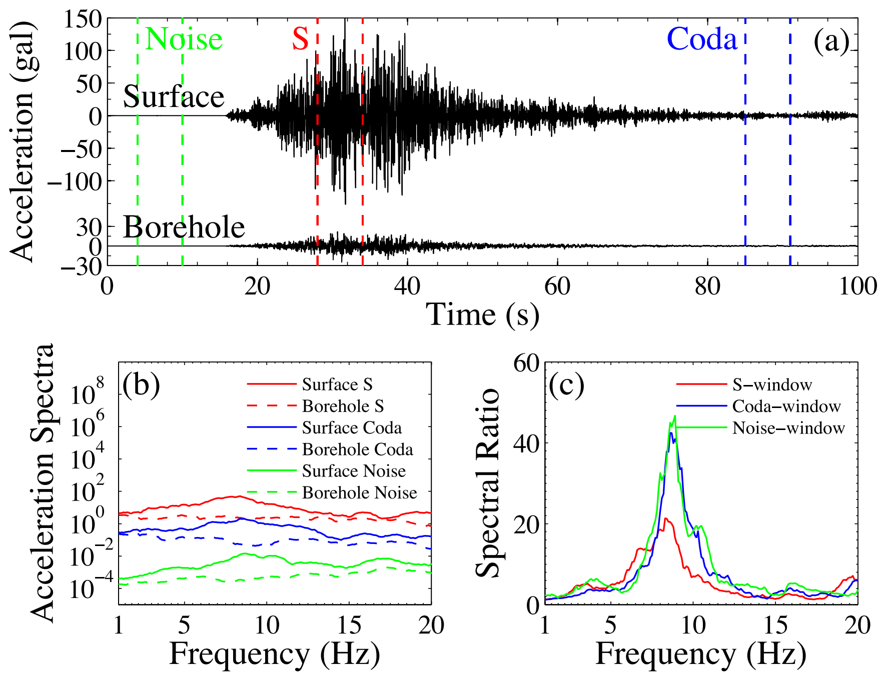

Fig. 3. (a) EW-component ground accelerations recorded at the station IBRH15 generated by an M_w 7.0 aftershock of Tohoku earthquake occurred on 04/11/2011. Surface and borehole recordings are shown at the top and bottom panels, respectively. The green, red and blue dashed lines indicate the pre-event noise, direct S and coda window that are used to compute the acceleration spectra in (b) and spectral ratios in (c).

tio traces for all the six stations from the sliding-window spectral ratio analysis. A general pattern observed from the spectral ratio traces is that the resonance frequency reduced sharply during the Tohoku main shock, followed by a recovery process (Fig. 4). The reference value of resonance frequency before the Tohoku earthquake is obtained by averaging all the resonance frequencies measured from the spectral ratio traces with PGA $<$ 100 Gal before the

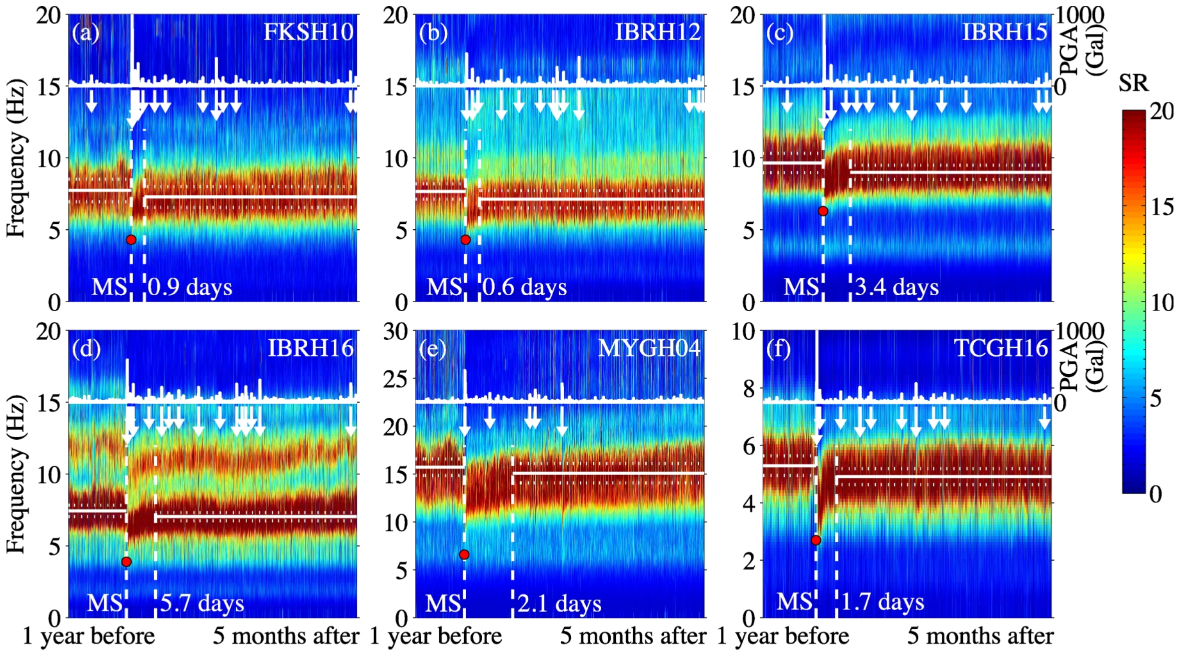

Fig. 4. Color-coded surface/borehole spectral ratios for the six stations. All the computed moving-window spectral ratios are aligned by the sequential number, rather than real time. The spectral ratio values are color-coded with red being high and blue being low. The two vertical dashed lines indicate the occurrence time of the Tohoku main shock, and the estimated time when most (95%) of the co-seismic changes are recovered. The horizontal solid and dotted lines show the reference value and uncertainties before and after the rapid recovery period defined as between the two vertical dashed lines. The white curve on the top of each panel shows the peak ground acceleration (PGA) value of the windowed seismogram used to compute the spectral ratio.

Tohoku main shock. Here we choose the threshold of 100 Gal to avoid the influences of significant nonlinear effects from moderate to large ground motions (Beresnev and Wen, 1996; Wu *et al.*, 2010).

Next, we estimate a rough recovery time by the following two steps: we first average the resonance frequencies measured from all the spectral ratios traces with PGA $<$ 100 Gal in the last month of data (07/12/2011–08/12/2011), and then we find the time point when the resonance frequency recover to 95% of the average resonance frequency in the last month. As shown in Fig. 4, the obtained time corresponds to the point where most (95%) of the co-seismic changes were recovered. In addition, we find that the average values in the last month after the main shock are always lower than those before the main shock. Hence, it is possible that either lower-amplitude longer-term recovery exists, and may continue after our analysis time period, or a permanent change occurs and will never return to the pre-main shock level.

3.2 Long-term recovery

To better quantify the post-seismic temporal change and potential longer-term recovery process, we stack the spectral traces in different time periods after the Tohoku main shock. As was done before (Wu *et al.*, 2009a), we divide the spectral ratios for each station into the following period: every month before the Tohoku main shock in linear time scale, and every 0.25 in the logarithmic time scale after the Tohoku main shock. We have tested different time windows for stacking the spectral ratio traces, and the obtained results are similar. We use logarithmic instead of linear time in the post-seismic period, mainly because previous studies have indicated logarithmic type of recovery process for the observed temporal changes in the shallow crust after the Tohoku earthquake (Nakata and Snieder, 2011; Wu and Peng, 2011). Next, we measure the resonance frequency of the stacked trace in each period.

As shown in Fig. 4, all the six stations show potential longer-term recovery within 5 months after the Tohoku main shock, and the slope of recovery at later time is not as steep as immediately after the main shock. In order to quantify whether longer-term recovery exist for each of the station, we compute the first-order polynomial (linear) least-squares fitting of the resonance frequencies after the end of Tohoku main shock recording. The main shock rupture time is generally around 150 s (Ammon *et al.*, 2011) and most strong shaking ends between 150–250 s (Suzuki *et al.*, 2011). Here we use 300 s after the Tohoku earthquake (vertical black dashed line in Fig. 5) to mark the end of the main shock and the starting time of the fit.

Next we compute the normalized Residual Standard Deviation (RSD) of measured resonance frequencies and the fitted line to determine the goodness of fit (Fig. 5). The RSDs for the stations FKSH10, IBRH12, and MYGH04 are lower than those for the other three stations, suggesting clear long-term logarithmic recovery at these sites. For stations IBRH15 and IBRH16, the RSDs are relatively higher because the resonance frequencies after 300 s are relatively flat. For station TCGH16, the RSD is relatively high because there is a clear change of recovery speed at $\sim 10^4$ s. Taking this into consideration, we divide the data into before and after 10^4 s and fit them separately (green dashed lines in Fig. 5(f)), which decrease the RSD from 0.23 to 0.06.

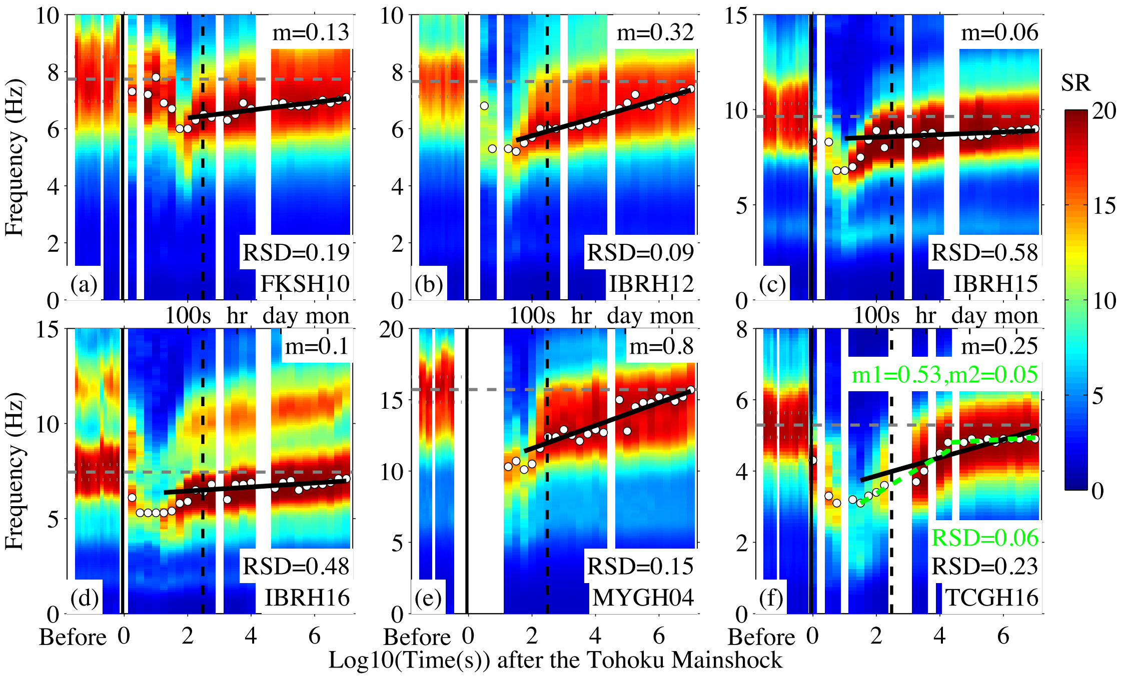

Fig. 5. Surface/borehole spectral ratios stacked in different time period before and after the Tohoku main shock for the six stations. The time periods are: every month before the Tohoku main shock in linear time scale, and every 0.25 in the logarithmic time scale after the Tohoku main shock. The stacked spectral ratio values are color-coded with red being high and blue being low. The vertical solid and dashed lines indicate the occurrence time of the Tohoku main shock, and the ending of Tohoku main shock record (~300 s). The horizontal solid and dotted grey lines show the reference value and uncertainties of the resonance frequency before the Tohoku main shock. The tilted black solid line is the least-squares fitting of the peak resonance frequencies after 300 s, which is projected back to the time when the highest PGA is recorded. The two green tilted dashed lines in panel (f) are the least-squares fittings of two stages of recovery within and after ~5 hours of the Tohoku main shock, respectively. The residual standard deviation (RSD) value and the slope of the regression line are shown in the bottom and top right corner of each panel, respectively.

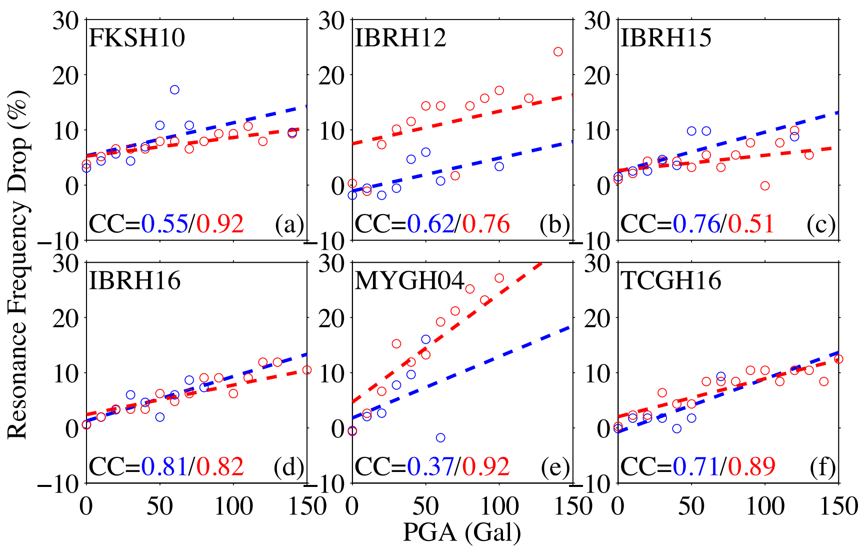

Fig. 6. Percentage drop of resonance frequency plotted against PGA for the six stations. The blue and red circles show the percentage drop of resonance frequency measured from stacked spectral ratio in each PGA bin before and after the Tohoku main shock, respectively. The blue and red dashed lines show the least-squares fitting of the blue and red circles, respectively. The correlation coefficient (CC) values are shown at the bottom of each panel.

3.3 Possible changes of susceptibility to further damages

To investigate whether the Tohoku earthquake has changed the susceptibility of near-surface material to further damages (e.g., Rubinstein and Beroza, 2004b), we check the slope between the resonance frequency drops and PGAs for all events before and after the main shock and use the slope as a proxy for damage susceptibility. The underlying assumption is that for a given PGA, material with higher degrees of damages would result in higher degrees of nonlinear response and larger reductions in resonance frequency (Vidale and Li, 2003; Rubinstein and Beroza, 2004b). In details, we divide the spectral ratios traces into three categories: before, during, and after the strong shaking and immediate recovery process caused by the Tohoku main shock (separated by the vertical solid and dashed lines in Fig. 4). The spectral ratios during the immediate recovery process (i.e., within 300 s of the Tohoku main shock) are not used here as they are dominated by the strong nonlinear effects and immediate fast recovery associated with the Tohoku main shock (Wu and Peng, 2011). We sort the spectral ratio traces before and after the major recovery process by their PGA values, and then average them in PGA bins of every 10 Gal from 0 Gal to 150 Gal. We have changed PGA bin width from 1 Gal to 20 Gal, and the obtained results are generally similar. Next, we measure the resonance frequency of the stacked trace at each PGA bin, and then compute the percentage drop of resonance frequency for each PGA bin before and after the recovery. Note that we use different reference values for the traces before and after the recovery when computing the percentage drop of resonance frequency (Fig. 5).

Figure 6 shows that at most sites the resonance frequency drops and the PGAs are correlated both before and after the main shock, as evidenced by their relatively high correlation coefficients (CCs). Based on the sites with high CCs (e.g., IBRH16 and TCGH16), we do not find a clear change of the slope between resonance frequency drop and PGA before and after the Tohoku main shock (Fig. 6). The resonance frequency drops for stations IBRH12 and MYGH04 are higher after the Tohoku main shock for most PGAs. This is likely because the reference level after the Tohoku earthquake is slightly overestimated due to the ongoing long-term recovery process, and this effect is particularly clear for stations IBRH12 and MYGH04 which show clearer long-term recovery than the other stations (Fig. 5).

4. Discussion

In this study, we found that longer-term (at least several months) lower-amplitude temporal changes of site response exist for all the six stations following a fast recovery at several hundred seconds to hours after the Tohoku main shock. The fitting slopes between the resonance frequency and the logarithmic time after the main shock for all six stations are positive, suggesting that the post-seismic recovery is still going on at the end of our analysis time period (5 month), rather than a permanent change. Our results are generally compatible with previous studies that have found logarithmic type of recovery of site response after large earthquakes in Japan (Sawazaki *et al*., 2006, 2009; Wu *et al*., 2009a; Nakata and Snieder, 2011; Wu and Peng, 2011) and elsewhere (Rubinstein and Beroza, 2004a; Peng and Ben-Zion, 2006; Wu *et al*., 2009b). However, the two-stage recovery processes have not been observed before. Specifically, Sawazaki *et al*. (2006, 2009) applied the sliding window spectral ratio technique to the KiK-Net data after the 2000 M_w 6.8 Western Tottori and 2003 M_w 8.3 Tokachi-Oki earthquakes and found quite different recovery time scale at different sites ranging from a few minutes to several years. Wu *et al*. (2009a) applied the same technique to the KiK-Net data after the 2004 M_w 6.6 Niigata earthquake, and found relatively short recovery time of several 10 s to more than 100 s at several sites. Nakata and Snieder (2011, 2012) applied a deconvolution technique to the data recorded at many KiK-Net stations and found logarithmic type of recovery after sharp reduction of S-wave velocity caused by the Tohoku main shock and other recent large earthquakes. Wu and Peng (2011) analyzed the KiK-Net data of the Tohoku main shock using the spectral ratio technique and found that the majority of resonance frequency drop is recovered within several hundreds of seconds after the Tohoku main shock, but they suggested that the recovery process was still going on at the end of the Tohoku main shock record.

The recovery time scale of at least several months found in this study is longer than tens of seconds found by Wu *et al*. (2009a) but shorter than several years found by Sawazaki *et al*. (2006, 2009). As suggested by previous studies, the recovery time scale is determined by the site condition, the input ground motion and other factors. We investigated the large PGAs after the Tohoku mainshock at the six sites but we do not find any correlation between frequency of large PGAs and the recovery time scale. Wu *et al*. (2009a) inferred that the variation in recovery time scale caused by site condition could be much more important than the input ground motion, as the recovery time scale observed at different sites under similar levels of ground motion could differ significantly. Wu and Peng (2011) investigated the velocity profiles of the six sites used in this study, and they found that the observed resonance frequencies in the spectral ratio traces (Figs. 4 and 5) generally match the values computed from the site profiles (Fig. 2). Here we re-analyzed the site profiles for the six stations from the KiK-Net website (http://www.kik.bosai.go.jp), including average S-wave velocity (V_{S30}) in the upper 30 m of the site (NEHRP, 2003), soil types at the sedimentary layers, and the S-wave velocity contrast. But we did not find a clear correlation between the site conditions and the recovery time scales. However, other aspects of site conditions (e.g., fluid system, permeability of the sedimentary rocks) could also play a role in determining the recovery time scale (Sawazaki *et al*., 2009; Wu *et al*., 2009a), but such information is not available at this stage.

Previous studies on temporal changes of soil properties after large earthquakes have identified several types of recoveries. Wu *et al*. (2009b) analyzed the spectral ratios between a pair of on- and off-fault stations along the North Anatolian fault after the 1999 Düzce earthquake in Turkey, and they found that the fault zone site response dropped $\sim$20–40 per cent and recovered with time scale of $\sim$1 day. However, because Wu *et al*. (2009b) use surface station pairs rather than borehole station pairs, the uncertainties in the average resonance frequency drops are relatively large, and they were not able to determine whether subtle long-term recovery exists or not after 1 day. On the other hand, other studies based on repeating earthquakes (e.g., Rubinstein and Beroza, 2004a; Schaff and Beroza, 2004; Peng and Ben-Zion, 2006) and ambient-noise or coda cross-correlation techniques (e.g., Brenguier *et al*., 2008; Nakata and Snieder, 2011) have found much longer-term but more subtle temporal changes (on the order of 0.1–5 per cent) in Turkey, California and Japan. Wu *et al*. (2009b) inferred that lack of identifiable repeating earthquakes immediately after the mainshock (e.g., in the first few hours) prevents the detection of larger co-seismic changes. Here we found large co-seismic changes in site response (on the order of a few tens per cent), rapid post-seismic recovery in the first few hundred seconds to several hours, and then a much longer-term slow recovery of at least five months (Fig. 5). We infer that this type of multiple-stage logarithmic recovery process may exist in other KiK-Net stations during the Tohoku sequence, as well as previous studies.

One possible explanation of our observations is the anomalous nonlinear fast dynamics and slow dynamics of the surface material. According to Johnson and Sutin (2005), sedimentary rocks typically belong to nonlinear mesoscopic material. When they are under high strain level ($>10^{-6}$) caused by seismic waves, the dynamic properties of rocks may behave in unexpected manners, which is typically manifested by shift of resonance frequency to lower value. This is also termed 'fast dynamics'. When the strain level drops after the seismic wave passed, the resonance frequency does not return to the pre-earthquake level immediately, but follows a logarithmic recovery within 10^3–10^4 s, also known as 'slow dynamics'. Although the spatial scales are much smaller in the laboratory experiment, the recovery time scale of 10^3–10^4 s is comparable to the time scale of several hundreds to several hours for the first stage of recovery observed in this study. For the second stage of long-term subtle recovery, previous studies have suggested that it might be associated with changes of fluid system (Sawazaki *et al.*, 2009; Wu *et al.*, 2009a), slow compacting, grain scale creeping, or other types of slow healing processes (Marone, 1998; Sleep *et al.*, 2000; N. Sleep, personal communication, 2012). When the strong ground motion increases the pore pressure, it caused a drop in shear modulus of the surface material and a reduction in resonance frequency. In this case, if the permeability of the sedimentary layers is relatively low, it would take a longer time to drain the excessive fluid after the strong shaking, and hence the recovery of the shear modulus also takes a longer time (Pavlenko and Irikura, 2002; Snieder and Beukel, 2004; Sawazaki *et al.*, 2009).

Wu and Peng (2011) found clear correlation between PGA and the observed resonance frequency drop during the Tohoku main shock. In this study we found that such correlation also exists for the moderate-size earthquakes before and after the Tohoku main shock (Fig. 6), which is consistent with the result of Wu *et al.* (2009a) on the 2004 Niigata earthquake sequence. In addition, we did not find clear changes of slopes between the PGAs and resonance frequency drops before and after the Tohoku main shock at least at the stations (IBRH16 and TCGH16) with high CC values. Hence we cannot conclude that the Tohoku main shock has increased the susceptibility to further damage, as originally proposed by Rubinstein and Beroza (2004b). We note that Rubinstein and Beroza (2004b) only measured temporal changes associated with one large aftershock (the M_l 5.4 Chittenden earthquake) of the M_w 6.9 Loma Prieta earthquake. So we cannot rule out the possibility that a similar-size earthquake before the Loma Prieta mainshock could also produce similar temporal changes. However, we also could not exclude the possibility that the change of susceptibility to further damage is too small and could bury in the uncertainties in our data. We leave this open for future studies.

Acknowledgments. We thank National Research Institute for Earth Science and Disaster Prevention (NIED) for providing the KiK-Net strong motion records of the 2011 Tohoku earthquake sequence. We thank Norm Sleep, an anonymous reviewer, and the editor Masanao Shinohara for their thorough review of the manuscript and useful comments. This work is partially supported by National Science Foundation (EAR-0909310) and Southern California Earthquake Center (SCEC). SCEC is funded by NSF Cooperative Agreement EAR-0106924 and USGS Cooperative Agreement 02HQAG0008.

References

Ammon, C. J., T. Lay, H. Kanamori, and M. Cleveland, A rupture model of the 2011 off the Pacific coast of Tohoku Earthquake, *Earth Planets Space*, **63**, 693–696, 2011.

Aoi, S., K. Obara, S. Hori, K. Kasahara, and Y. Okada, New Japanese uphole/downhole strong-motion observation network: KiK-net, *Seismol. Res. Lett.*, **72**, 239, 2000.

Beresnev, I. and K. Wen, Nonlinear soil response-A reality?, *Bull. Seismol. Soc. Am.*, **86**, 1964–1978, 1996.

Bonilla, L. F., K. Tsuda, N. Pulido, J. Régnier, and A. Laurendeau, Nonlinear site response evidence of K-NET and KiK-net records from the 2011 off the Pacific coast of Tohoku Earthquake, *Earth Planets Space*, **63**, 785–789, 2011.

Brenguier, F., M. Campillo, C. Hadziioannou, N. Shapiro, R. Nadeau, and E. Larose, Postseismic relaxation along the San Andreas fault at Parkfield from continuous seismological observations, *Science*, **321**, 1478, 2008.

Chin, B. and K. Aki, Simultaneous study of the source, path, and site effects on strong ground motion during the 1989 Loma Prieta earthquake: A preliminary result on pervasive nonlinear site effects, *Bull. Seismol. Soc. Am.*, **81**, 1859–1884, 1991.

Frankel, A., D. Carver, and R. Williams, Nonlinear and Linear Site Response and Basin Effects in Seattle for the M 6.8 Nisqually, Washington, Earthquake, *Bull. Seismol. Soc. Am.*, **92**, 2090–2109, 2002.

Goldstein, P., D. Dodge, M. Firpo, and L. Minner, SAC2000: Signal processing and analysis tools for seismologists and engineers, in *In The IASPEI International Handbook of Earthquake and Engineering Seismology, Part B, Chap 85.5*, edited by W. H. K. Lee, H. Kanamori, P. C. Jennings, and C. Kisslinger, Academic Press, London, 2003.

Hirose, F., K. Miyaoka, N. Hayashimoto, T. Yamazaki, and M. Nakamura, Outline of the 2011 off the Pacific coast of Tohoku Earthquake (M_w 9.0)—Seismicity: foreshocks, mainshock, aftershocks, and induced activity—, *Earth Planets Space*, **63**, 513–518, 2011.

Johnson, P. and A. Sutin, Slow dynamics and anomalous nonlinear fast dynamics in diverse solids, *J. Acoust. Soc. Am.*, **117**, 124–130, 2005.

Joyner, W., R. Warrick, and A. Oliver, Analysis of seismograms from a downhole array in sediments near San Francisco Bay, *Bull. Seismol. Soc. Am.*, **66**, 937–958, 1976.

Marone, C., Laboratory-derived friction laws and their application to seismic faulting, *Ann. Rev. Earth Planet. Sci.*, **26**, 643–696, 1998.

Nakata, N. and R. Snieder, Near-surface weakening in Japan after the 2011 Tohoku-Oki earthquake, *Geophys. Res. Lett.*, **38**, L17302, 2011.

Nakata, N. and R. Snieder, Estimating near-surface shear wave velocities in Japan by applying seismic interferometry to KiK-net data, *J. Geophys. Res.*, **117**, B01308, doi:10.1029/2011JB008595, 2012.

NEHRP, NEHRP recommended provisions for seismic regulations for new buildings and other structures (FEMA 450), in *National Earthquake Hazards Reduction Program (NEHRP), Building Seismic Safety Council*, Washington, DC, 2003.

Pavlenko, O. and K. Irikura, Changes in shear moduli of liquefied and nonliquefied soils during the 1995 Kobe Earthquake and its aftershocks at three vertical-array sites, *Bull. Seismol. Soc. Am.*, **92**, 1952–1969, 2002.

Peng, Z. and Y. Ben-Zion, Temporal changes of shallow seismic velocity around the Karadere-Düzce Branch of the North Anatolian Fault and strong ground motion, *Pure Appl. Geophys.*, **163**, 567–600, 2006.

Rubinstein, J., Nonlinear site response in medium magnitude earthquakes near Parkfield, California, *Bull. Seismol. Soc. Am.*, **101**, 275–286, 2011.

Rubinstein, J. and G. Beroza, Evidence for widespread nonlinear strong ground motion in the MW 6.9 Loma Prieta Earthquake, *Bull. Seismol. Soc. Am.*, **94**, 1595–1608, 2004a.

Rubinstein, J. and G. Beroza, Nonlinear strong ground motion in the ML 5.4 Chittenden earthquake: Evidence that preexisting damage increases susceptibility to further damage, *Geophys. Res. Lett.*, **31**, L23614, doi:10.1029/2004GL021357, 2004b.

Sawazaki, K., H. Sato, H. Nakahara, and T. Nishimura, Temporal change in site response caused by earthquake strong motion as revealed from coda spectral ratio measurement, *Geophys. Res. Lett.*, **33**, L21303, doi:10.1029/2006GL027938, 2006.

Sawazaki, K., H. Sato, H. Nakahara, and T. Nishimura, Time-lapse changes of seismic velocity in the shallow ground caused by strong ground motion shock of the 2000 Western-Tottori Earthquake, Japan, as revealed from coda deconvolution analysis, *Bull. Seismol. Soc. Am.*, **99**, 352–366, 2009.

Schaff, D. and G. Beroza, Coseismic and postseismic velocity changes measured by repeating earthquakes, *J. Geophys. Res.*, B10302, 2004.

Sleep, N., E. Richardson, and C. Marone, Physics of friction and strain rate localization in synthetic fault gouge, *J. Geophys. Res.*, **105**, 25875–25890, 2000.

Snieder, R. and A. Beukel, The liquefaction cycle and the role of drainage in liquefaction, *Granular Matter*, **6**, 1–9, 2004.

Suzuki, W., S. Aoi, H. Sekiguchi, and T. Kunugi, Rupture process of the 2011 off the Pacific coast of Tohoku earthquake derived from strong-motion data, Japan Geoscience Union Meeting MIS036-P043, Makuhari, Chiba, Japan, May 022–027, 2011.

Vidale, J. and Y. Li, Damage to the shallow Landers fault from the nearby Hector Mine earthquake, *Nature*, **421**, 524–526, 2003.

Wen, K., Non-linear soil response in ground motions, *Earthq. Eng. Struct. Dyn.*, **23**, 599–608, 1994.

Wu, C. and Z. Peng, Temporal changes of site response during the 2011 M_w 9.0 off the Pacific coast of Tohoku Earthquake, *Earth Planets Space*, **63**, 791–795, 2011.

Wu, C., Z. Peng, and D. Assimaki, Temporal changes in site response associated with strong ground motion of 2004 Mw 6.6 Mid-Niigata earthquake sequences in Japan, *Bull. Seismol. Soc. Am.*, **99**, 3487–3495, 2009a.

Wu, C., Z. Peng, and Y. Ben-Zion, Non-linearity and temporal changes of fault zone site response associated with strong ground motion, *Geophys. J. Int.*, **176**, 265–278, 2009b.

Wu, C., Z. Peng, and Y. Ben-Zion, Refined thresholds for nonlinear ground motion and temporal changes of site response associated with medium size earthquakes, *Geophys. J. Int.*, **183**, 1567–1576, doi:1510.1111/j.1365-1246X.2010.04704.x, 2010.

Yu, G., J. Anderson, and R. Siddharthan, On the characteristics of nonlinear soil response, *Bull. Seismol. Soc. Am.*, **83**, 218–244, 1992.

C. Wu (e-mail: cwu@lanl.gov) and Z. Peng